Planta (2006) 223: 755–768
DOI 10.1007/s00425-005-0136-5

ORIGINAL ARTICLE

M. Bastida · E. Graziano · R. Roca · I. López
N. Sánchez-Pons · P. Puigdoménech · C. M. Vicient

A maize defective-kernel mutant (*longcell*) characterized by tubular cells, severe morphological alterations and induction of cell death

Received: 9 May 2005 / Accepted: 15 August 2005 / Published online: 18 October 2005

Abstract Seeds of the *longcell* mutant in maize (*Zea mays* L) have a defective-kernel phenotype: the embryo aborts at the early coleoptilar stage and the endosperm is reduced in size. Mutant embryos have severe alterations in morphogenesis. They have a suspensor-, an embryo axis- and a scutellum-like structure, but the shoot apical meristem (SAM) is not formed. Scanning electron microscopy showed that most of the cells in *longcell* embryos are tubular and abnormally enlarged. The level of expression of several genes involved in basic metabolism is not severely affected during early and mid embryogenesis, but storage molecule accumulation is reduced. Genes which in normal conditions are only expressed after germination, are expressed during kernel development in the *longcell* seeds. Mutant embryos undergo cell death in late embryogenesis. Nuclei in dying embryos are TUNEL positive, and different genes coding for hydrolytic enzymes are up-regulated. The expression of genes related to oxidative stress is also altered in *longcell* embryos. These results lead us to suggest that the *longcell* mutant may be cytokinesis-defective.

Keywords Cell death · Defective kernel mutants (*dek*) · Embryo development · *Zea*

Abbreviations PCD: Programmed cell death · MIPS: Myo-inositol 1-phosphate synthase · Dap: Days after pollination

M. Bastida · E. Graziano · R. Roca · I. López
N. Sánchez-Pons · P. Puigdoménech · C. M. Vicient (✉)
Laboratori de Genetica Molecular i Vegetal, CSIC-IRTA,
Jordi Girona 18-36, 08034 Barcelona, Spain
E-mail: cvsgmp@cid.csic.es
Tel.: +34-93-4006100
Fax: +34-93-2045904

Introduction

Embryogenesis is a complex, coordinated process that leads to the transformation of a single-cell zygote into an embryo (Jürgens 2001). It is usually divided into three main periods: early embryogenesis (proembryo to transition), during which the fertilized egg goes through a series of cell divisions in which a radially symmetric proembryo differentiates into a club-shaped structure, with an embryo proper and a suspensor; mid-embryogenesis (coleoptilar stage), during which the embryo acquires bilateral symmetry, with an embryo axis and a scutellum, and then produces the radicle, coleoptile and the first leaf primordium; and late embryogenesis, during which the embryo axis differentiates up to six leaf primordia, reserves are accumulated and dormancy is established.

Cell division orientation is important in the regulation of plant embryogenesis (Jürgens 2001). In *Arabidopsis*, the orientation of cell divisions in the embryo is precisely determined, and alterations in cytokinesis result in severe modifications in morphogenesis, and sometimes cell death (Söllner et al. 2002). In contrast, the orientation of cell divisions in maize during early embryo development is not so strictly conserved and only becomes essential in mid-embryogenesis, with the establishment of bilateral symmetry and organ definition (Ingram et al. 2000). Maize embryo mutants with irregular patterns of cell division have been described as not being able to pass the transition stage (Consonni et al. 2003).

Embryo lethality is one of the most common mutant traits in plants (Meinke et al. 2003; Magnard et al. 2004). In maize, embryo lethal mutants have been classified as *embryo defective* (*emb*), which produce a distorted embryo with no endosperm defects, and *defective kernel* (*dek*), that have an effect in both the embryo and endosperm (Sheridan and Clark 1993). A number of *dek* and *emb* genes have been cloned. *Dek1* encodes a calpain protein involved in signal transduction (Lid et al. 2002),

the *emb8516* mutant is produced by an insertion in the *ZmPRPL35* gene encoding a plastid ribosomal protein (Magnard et al. 2004; Ma and Dooner 2004), and the *empty pericarp 2* (*emp2*) mutant is produced by an insertion in a gene encoding a heat shock binding protein (HSBP1) (Fu et al. 2002).

Programmed cell death (PCD) is a genetically controlled, active process that results in the death of individual cells, tissues, or whole organs. It has been associated with several processes in plants, including several environmental responses (Lam and Greenberg 2000). PCD is an essential morphogenetic mechanism in the development of plants and is involved, for example, in the differentiation of tracheary elements, differentiation of sexual organs, determination of leaf shape or in senescence. PCD is also involved in seed development in the seed coat, nucellus, suspensor, endosperm, aleurone layer and scutellum (Gallie 2004).

A number of maize mutants have been isolated by Dellaporta and Moreno (1994) by transposon insertion. One of these mutants, which we have called *longcell*, has a distorted embryo and a reduced endosperm, and it is a lethal and recessive mutation (Graziano et al. 2003). Here we describe the phenotypic, biochemical and molecular characterization of the *longcell* mutant, including the isolation of differentially expressed genes by DD-RT, and we studied how the mutation affects the expression of several other genes.

Material and methods

Biological material

The maize *longcell* mutant was produced by Dellaporta and Moreno (1994). Wild type maize corresponds to *Zea mays* L cv W64A pure inbred line and was originally obtained from the ''Estacion Experimental de Aula Dei'' (CSIC, Zaragoza, Spain). Seeds of the *Vp1* mutant were obtained from the Maize Genetics Cooperative Stock Center. All the plant lines used were grown in the greenhouses of the IBMB-CSIC in Barcelona, Spain.

In vitro culture

For embryo rescue, ears were harvested between 12 and 30 days after pollination, surface sterilized with 5% (w/v) sodium hypochlorite for 15 min and then rinsed in sterile, distilled water. Embryos were removed aseptically and transferred to MS medium (pH 5.6) and 0.8% agar (w/v). Cultures were incubated in a growth chamber at 25°C in continuous dark. Germination was controlled 5, 15 and 30 days after culture. For callus regeneration, immature sterile embryos were placed on MS medium (pH 5.6) supplemented with vitamins (Sigma), sucrose (20 g l^{-1}), 2,4-D (1 mg l^{-1}) and agar (2 g l^{-1}), and cultured in a growth chamber at 25°C in continuous dark. Callus formation was controlled 30 days after culture.

Scanning electron microscopy

Maize embryos were fixed in ethanol, formaldehyde, acetic acid (80:3.5:5; by vol) for 30 min at room temperature. After fixation the samples were transferred to 70% ethanol and taken through an alcohol dehydration series. The dehydrated specimens were immersed for 10 min in mixtures of ethanol/isoamyl acetate (2:1, 1:1 and 1:2, v/v), and finally three times in 100% isoamyl acetate. Dehydrated material was critical point dried using liquid CO_2 and transferred to the Fine Coat Ion Sputter JFC-100 (Jeol) vacuum preparation chamber for supttering. The conditions used were 10^{-1} Torr, 20 mA, 1 kV and mounted at a distance of aproximately 3 cm from the sample surface. Argon sputtering was performed for 4 min. After sputtering, the samples were sputter-coated with 400 Å gold. Samples were examined in a Hitachi S2300 scanning electron microscope from ''Serveis Científico-Tècnics'' (Universitat de Barcelona).

Optical microscopy, in situ mRNA hybridization and TUNEL assay

Embryos and kernels at different developmental stages were collected and fixed in an ethanol:formaldehyde:acetic acid (80:3.5:5; by vol) fixative solution for 1 h at room temperature, followed by 1 week at 4°C. Once fixed, the material was stored in 70% ethanol at 4°C. Paraffin inclusion, sectioning and mRNA hybridizations were according to Langdale (1994) using an RNA colour kit for non-radioactive in situ hybridization (Amersham). Digoxigenin labelled hybrids were viewed using bright field microscopy. Starch staining was done using the iodine–potassium iodide method (IPI): 2% KI + 0.2% I_2 in water for 30 s. For TUNEL assays, the tissues were treated with the ''In Situ Cell Death Detection'' kit (Roche Molecular Biochemicals) according to the supplier's protocol for difficult tissues. For aleurone staining, mature grains were fixed overnight at room temperature in 2% glutaraldehyde/0.3 M sodium-phosphate buffer (pH 6.5). Hand cut sections were stained for neutral lipids with a saturated ethanol 95% solution of Sudan red 7B.

RT-PCR analyses

Total RNAs were treated with DNAse I (RNAse-free DNAseI, Promega). Total pre-treated RNA (2 μg) was reverse transcribed with the Omniscript reverse transcriptase kit (Qiagen) using an oligo-dT primer. cDNAs were amplified with specific primers, designed flanking introns (see Table. 1, 2). Controls with non-reverse

Table 1 Genes used in expression analyses

Protein	Gene	GeneBank Acc. Numb.	Primer 5′	Primer 3′	Reference
α-Amylase	AMY	L25805	GCATCTACTGCGTCTTCGAGGGC	CCTTGGTGGTGAAGTCGAACGCC	Young et al. (1994)
B-D-Glucanase	BDG	U33816	GCCAGTGGTTCGTGGTGACTACCC	GCCATAACGTTCGGTGAAGCCGGC	Brzobohaty et al. (1993)
S1 type endonuclease 1	MEN1	AI920711	AGCAAGGGATGTGCGTCGTCGGGG	CCCAGTGGACGATGTCGTCAGACC	Aoyagi et al. (1998)
Vacuolar aspartic proteinase (Phytepsin)	Phyt	TC233934	GGGACTTCATTGCTTGCTGGTCC	GCCCTAATCCTCATCGTCTCCCT	Runeberg-Roos and Saarma (1998)
Subtilisin-like serine protease	SAS1	CG301284	TGCTCCAGTACATACGGAGCAGC	GTGCAGCAGTGTAGTTCATGGCG	Coffeen and Wolpert (2004)
Metacaspase Ia	McIa	BG320767	TCTGCAAGGGCACGAGCGGCGGC	CTCGCATTCCACCGCCTTGATG	Uren et al. (2000)
Metacaspase Ib	McIb	BI679471	TCTGGAAAGGCACTAGTGGTGGG	GAACACGTCATAGGGAGAAGGGC	Uren et al. (2000)
Metacaspase IIa	McIIa	BM079161	GCGATGAGCATGTTCATGTCGC	GGTACAGATCACGATACAAGTGTG	Uren et al. (2000)
Metacaspase IIb	McIIb	BG518394	AGCGATGAGAATGCCAGTGCG	TGCGAAAGAAACGATACATTCCC	Uren et al. (2000)
Peroxirredoxin	Per	AW231778	CGGTAGTGCCACGAACCGGTTGCC	CATCCACGACTACGTCGGCGACGG	Stacy et al. (1996)
Metallothionein-like protein 1	Met1	S57628	CTGACCTGGAGGAGACGAGCA	CATGAGCACAAAGACTGACGCC	de Framond (1991)

Table 2 Identification of DDRT cDNA clones and their similarities to known genes

Band	Size (bp)	Overexpressed in	Best Hit (blast nucleotide)	Gene	Accession number	*E* value	5′ primer	3′primer	Reference
LCD1	411	Wild type	Myo-inositol 1-phosphate synthase	MIPS	AF056326	0.0	CCACTTCCCGGTGTCTATGATCCG	GGTTCATGCCGTCGTTGTTTCCC	Shuckla et al. (2004)
LCU1	284	*longcell*	*Oryza sativa* cytochrome b245 *β*-chain, NADpH Oxidase	NAD	X93301	7e-84	GTGACCACTGCAAAAGGCGCTGC	GTCCTCTCCCCTACATACAGGCC	Keller et al. (1998)
LCD2	274	Wild type	*Oryza sativa* pectate lyase-like protein	PL	BAB89233	3e-21	CTCACCGGCAAGGGGCTCCAGCTC	ATCGATCAGCGAGGGCAGCGCGCC	Turcich et al. (1993)
LCD3	199	Wild type	Histone deacetylase 2b	HD2b	AAF68624	6e-34	GAAGCTTGCCATTGGAACGCTCTC	TTCGTCAGGAGATAATCCCTCGCC	Zhou et al.(2004)
LCD4	118	Wild type	Cyclophilin	Cyp	X68678	2e-44	CTCGCGTCTTCTTCGACATGACCG	CCTTGACCACCTTGGAGGTGGAGC	Marivet et al. (1995)

transcribed RNA were also used to detect gDNA contamination. The ubiquitin gene was used as a control for RNA loading. PCR reactions were performed using 0.2 mM each dNTP, 360 μg ml^{-1} BSA and 1 pmol μl^{-1} of each primer in a final volume of 50 μl. The reaction mixtures were heated to 95°C for 5 min, followed by repeated cycles of 94°C for 30 s, 55°C for 30 s, and 72°C for 90 s. Reactions were completed with an incubation at 72°C for 10 min. Reactions were performed in a Minicycler (MJ Research, Waltham, MA, USA) thermal cycler. The amounts of template cDNA and the number of PCR cycles were determined for each gene to ensure that amplification occurred in the linear range and allowed good comparison of the amplified products. At least three independent analyses were carried out on the different RNA samples.

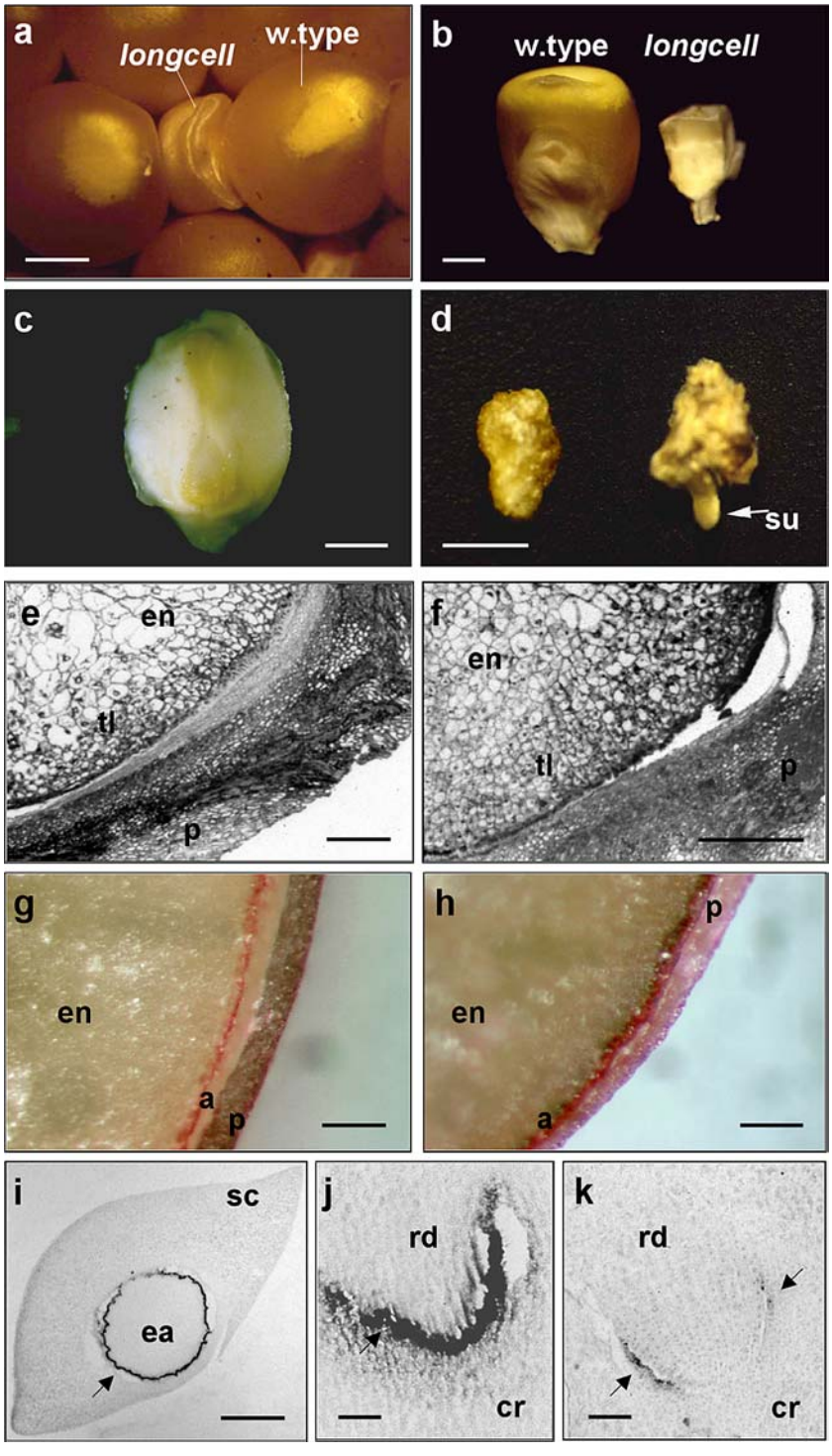

Fig. 1 **a**–**k** Effects of *longcell* mutation on seed and embryo development. **a** Kernels of self-pollinated ears of a *longcell* heterozygous plant. **b** Wild type and *longcell* mature kernels, adaxial side. **c** Wild type embryo dissected from dry seed. **d** *longcell* mutant embryos dissected from dry seeds. The *arrow* indicates the suspensor-like structure. **e, f** Longitudinal section of a 20 dap wild type (**e**) and *longcell* (**f**) kernel showing the basal endosperm transfer layer. **g, h** Longitudinal sections of wild type (**g**) and *longcell* (**h**) dry seeds stained with Sudan Red 7B showing the aleurone layer in red. **i–k** In-situ hybridization showing the mRNA accumulation pattern of malic enzyme (*EM*) in sections of 20 dap immature embryos. **i** Wild type transversal section; **j** wild type longitudinal section; **k** *longcell* longitudinal section. *Arrows* indicate the hybridization. *su* suspensor, *tl* basal endosperm transfer layer, *en* endosperm, *p* pericarp, *a* aleurone layer, *sc* scutellum, *rd* radicle, *cr* coleorhyza, *ea* embryo axis. *Bars* represent 2 mm (**a**, **b**), 1 mm (**c**, **d**), 200 μm (**e**–**h**), 150 μm (**i**), 60 μm (**j**) and 40 μm (**k**)

Biochemical and activity analysis of maize kernels

Crude protein extracts were made from dry seeds of the different maize lines or from seedlings 1 day after germination, by grinding in 2 ml of soluble extraction buffer, containing 40 mM NaAc (pH 4.8), 20 mM $CaCl_2$, and 60 mM NaCl, in a pestle and mortar. Samples were centrifuged at 14,000*g* for 10 min to pellet insoluble material, heated at 70°C for 15 min and centrifuged again at 8,000*g* for 5 min at 4°C. The protein concentration was measured using the Bradford method (Bradford 1976). Amylase activity was determined by measuring the reduction in the starch content of the reaction mix after incubation at 37°C for 30 min. Reaction mix consisted in 50 µl of protein extract and 400 µl of reaction buffer: 50 mM NaAc (pH 4.8), 20 mM $CaCl_2$, 60 mM NaCl and 0.3% soluble starch (w/v). Starch content was measured using the iodine method (Halick and Keneaster 1956). Activity was estimated against a standard and expressed as mg starch degraded per min per mg of extracted protein.

Identification of differentially expressed genes

RNAs were obtained from 20 day after pollination (dap) wild type and *longcell* maize seeds, dissected from the same heterozygous ears. Differential display procedures were carried out as described by Bastida and Puigdomenech (2002). Reverse transcription was performed on 0.2 µg of total RNA, using a T_{12}MN oligonucleotide as anchor-primer. Two microliters of this cDNA were used as template for the polymerase chain reaction (PCR), in which an arbitrary decamer oligonucleotide was used in combination with the T_{12}MN oligonucleotide. Products were labelled with ^{35}S-dATP and separated on a denaturing polyacrylamide gel. This gel was exposed to X-ray film, and the bands of interest cut out, amplified with the same combination of oligonucleotides and cloned into a pGEM-T vector (Promega, Madison, WI, USA). To prevent isolation of false positives, all amplification experiments were performed twice for each primer combination. Only those cDNA bands whose levels of expression were affected in both reactions were selected for further analysis.

Results

Phenotype of *longcell* kernels and storage molecule accumulation

The mutant line described here was obtained using the strategy of gene tagging by the Activator (Ac) transposon (Dellaporta and Moreno 1994). The *longcell* mutation behaves as a Mendelian recessive trait. Heterozygous plants are not visibly abnormal at the vegetative stage. Homozygous mutant kernels are characteristically small, with a reduced endosperm (Fig. 1a, b) (Graziano et al. 2003). Mutant kernels have an average weight of 54.3 mg/kernel, while in the wild type the average is 173.3 mg/kernel, in our culture conditions. Examination of the embryos showed that although they are variable in shape they always have a rough surface and are blocked between the late transition and early coleoptilar stage (Fig. 1c, d). Although the endosperm is reduced in size, it has the typical vitreous texture, basal endosperm transfer layer (Fig. 1e, f) and aleurone layer (Fig. 1 g, h), and the pericarp in *longcell* kernels is not altered (Fig. 1 g, h). Despite their abnormal shape, mutant embryos often have suspensor-, scutellum-, embryo axis- and radicle-like structures, but

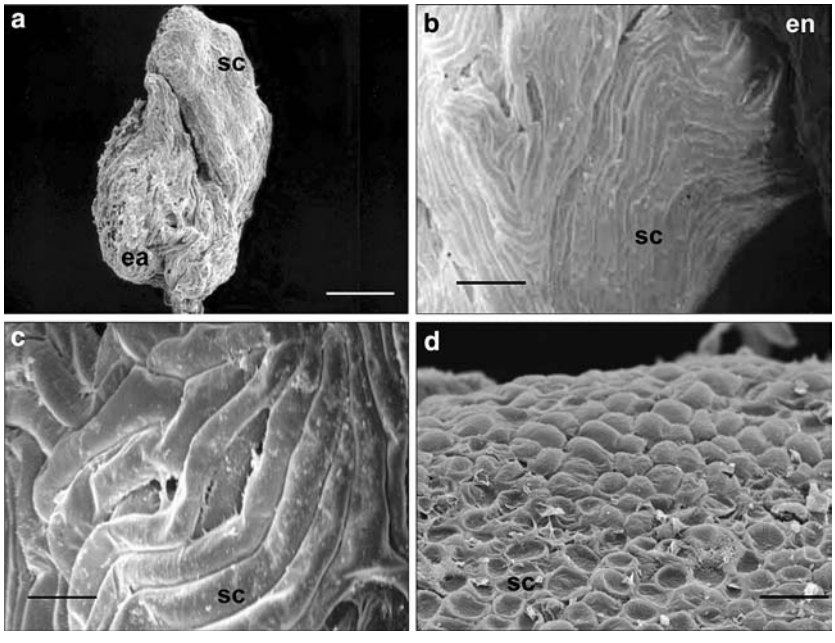

Fig. 2 **a**–**d** Enlarged cells on the surface of mutant embryos. Scanning electromicrographs of dissected *longcell* (**a**, **b**, **c**) and wild type (**d**) immature embryos (30 dap) showing the different cell shape on the surface of the scutellum. *sc* scutellum, *ea* embryo axis-like, *en* endosperm. *Bars* represent 0.5 mm (**a**), 200 µm (**b**) and 60 µm (**c, d**)

they never develop a shoot apical meristem (SAM). Cells in the scutellum-like structure are bigger and more irregular in shape than in the embryo axis-like structure. The differentiation of the radicle is shown by the analysis of expression of a gene coding for a malic enzyme (EM). In wild type embryos, this gene is specifically expressed in the epidermis of the radicle (Fig. 1i, j) (Lopez-Becerra et al. 1998), and 20 dap *longcell* embryos accumulate EM mRNA in a position equivalent to the epidermis of the radicle (Fig. 1k). Mutant embryos did not germinate in vitro or generate callus under our experimental conditions (see Material and methods).

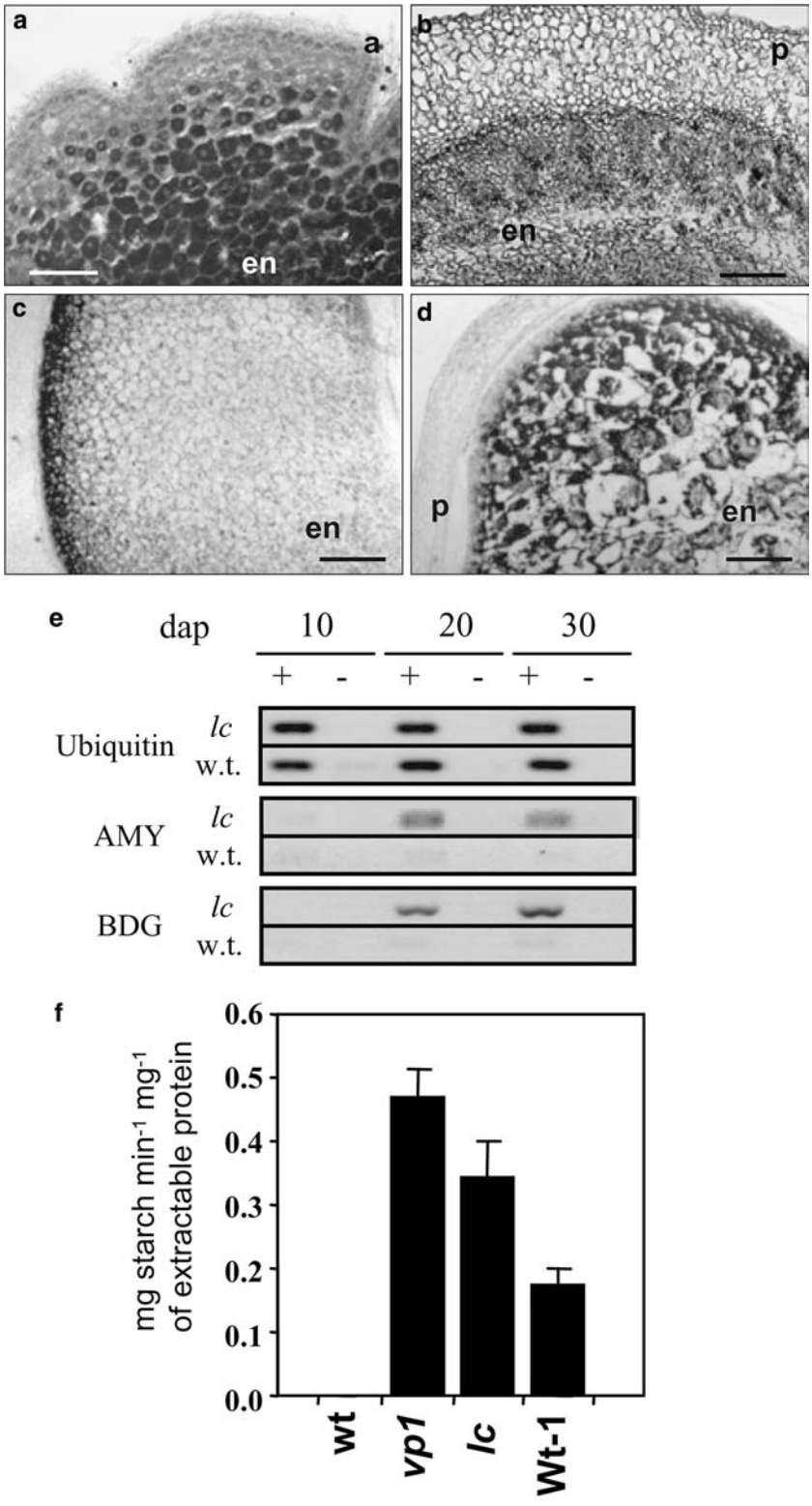

Fig. 3 **a**–**f** Accumulation of reserves and expression of the post-germination gene program during embryogenesis in *longcell* mutants. **a**–**b** IPI starch staining of wild type (**a**) and *longcell* endosperm (**b**) in dry seeds showing the dark starch staining. **c-d** mRNA accumulation pattern of *γ-zein* in transversal sections of 20 dap wild type (**c**) and *longcell* (**d**) kernels. *en* Endosperm, *p* pericarp, *a* aleurone layer. *Bars* represent 100 μm (**a, c, d**) and 60 μm (**b**). **e** RT-PCR analysis of the expression profiles of two germination specific maize genes. Ethidium bromide-stained 1.5% agarose gels showing RT-PCR products. Details of the genes are given in Table 1. AMY is *α-amylase* and BDG is *β-D-glucanase*. *lc* corresponds to *longcell* kernels and w.t. to wild type. The numbers at the top correspond to days after pollination. In each case, the size of the bands shown are those expected. The ubiquitin gene was used as control. + Corresponds to the RT-PCR assays and, − to the negative controls in which the reverse transcriptase was not included in the reaction. **f** Comparison of α-amylase activity in dry and germinating seeds of wild type and selected mutants. *Wt* Wild type, *Vp1 viviparous 1, lc longcell, wt-1* wild type seeds 1 day after germination

Scanning electron microscopy shows that cells on the surface of *longcell* embryos are abnormally long (Fig. 2a, b, c) compared to the wild type (Fig. 2d). The enlarged cells are about 500 μm long and are enlarged allometrically, expanding only along the longitudinal axis. The first appearance of enlarged cells is around 20 dap in the region corresponding to the scutellum-like structure, next to where the SAM should be, and this spread throughout the embryo.

To further characterize the mutant kernels, the starch content was quantified. The amount of starch is lower in *longcell* kernels: 21 fold lower expressed in amount of starch per seed, and 5.7 fold lower calculating the content per weight of flour. The same conclusion was observed when sections of mutant seeds where treated with iodine–potassium iodate (IPI), which stains starch black (Fig. 3a, b). As expected, a strong black signal was observed in wild type seeds, but was very much reduced in the mutant endosperm under the same reaction conditions. Extractable proteins were also quantified. As expected due to the reduced size of the seed, the amount of protein per seed is lower in *longcell* kernels (1.4-fold lower for extractable proteins and 21-fold for starch). However, calculating the content per weight of flour, the amount of extractable proteins is 2.3 fold higher in the mutant. This can at least partially be explained by the reduced contribution of the starch to the final weight of the seed.

We also found some differences between mutant and wild type kernels when we examined the pattern of mRNA accumulation of the *γ-zein* gene, which codes for a storage protein. During normal development, *γ-zein* mRNA accumulates in high concentrations in the first few layers of subaleurone cells in the endosperm (Geetha et al. 1991; Fig. 3c). In situ hybridization with a probe for the *γ-zein* gene product showed that, in the *longcell* mutants, *γ-zein* mRNA is accumulated in both the subaleurone and central endosperm cells (Fig. 3d). This suggests a more general distribution of *γ-zein* in the mutant endosperm.

Many hydrolytic enzymes are expressed in the scutellum and aleurone layers during germination. In normal conditions, *α-amylase* mRNA, protein and activity are only detected a few hours after germination (Chandler et al. 1984). We designed PCR primers specific for the *α-amylase* gene (Table 1) and analyzed the mRNA accumulation by RT-PCR analysis. As expected, the *α-amylase* gene was not expressed in the wild type during kernel development (Fig. 3e) but in the mutants, *α-amylase* transcripts were found at 20 and 30 dap. We examined the accumulation of the *β-D-glucanase* mRNA (Table 1), which is only expressed after germination in normal conditions, but in *longcell* kernels we detected the mRNA from 20 dap. We also examined the α-amylase activity in dry seeds of wild type, *longcell* and *Vp1* lines, as well as wild type seeds 1 day after germination (1 dag) (Fig. 3f). The α-amylase activity was higher in germinating compared to dry, wild type seeds, and also higher in the *Vp1* mutant, as has been previously described (Young and Gallie 2000). Higher activity is also observed in *longcell* seeds, which correlates well with the expression of the gene during seed development.

Differences in the mRNA accumulation of embryo marker genes

The isolation of several marker genes, characteristically expressed during different processes that take place during embryogenesis, allows us to evaluate which mechanisms are affected in the embryo of *longcell* mutants. We examined the mRNA accumulation of several of these genes, from different functional categories, in wild type and *longcell* embryos at different stages of development (Fig. 4).

The first category of genes examined was those involved in cell division. Two genes were examined, one coding for the histone 3 (H3), and a second coding for the translation elongation factor 1α (EF-1α). These genes are preferentially expressed in those parts of the embryo in which cell division is more frequent, such as the epidermis of the scutellum, meristems and provascular tissues. In the wild type, H3 mRNA has a characteristic "spotted" distribution because its expression is only high during cell division (Fig. 4a, b), whereas EF-1α mRNA does not have this type of distribution, because its expression is high throughout the cell cycle in proliferating tissues (Fig. 4e). In 20 dap *longcell* embryos, both mRNAs accumulate but with a no organized pattern (Fig. 4c, g). EF-1α mRNA is accumulated in certain regions of 12 dap embryos (Fig. 4f).The expression of both genes in 35 dap *longcell* embryos is reduced to a few scattered cells (Fig. 4d, h).

We also examined the mRNA accumulation of genes involved in basic cell metabolism with a gene coding for glyceraldehyde phosphate dehydrogenase (GPD) (EC 1.2.1.13) involved in glucolysis, a gene coding for an acyl carrier protein (AP17) involved in lipid biosynthesis (Roca et al. 1998), and a gene coding for a clathrin adapter protein (CAP) involved in vesicle transport from the Golgi apparatus. In wild type embryos, all three genes share a similar pattern of mRNA accumulation, with a basal level of expression throughout the embryo, a high level of mRNA accumulation in the epidermis and subepidermal layers of the scutellum, and a gradient of mRNA abundance decreasing towards the embryo axis (Fig. 4i, m, q). Despite the morphological alterations, all three genes are similarly expressed in 12 and 20 dap *longcell* embryos. At 12 dap the expression of all three genes is general in the embryo proper and absent in the suspensor (Fig. 4j,n,r). At 20 dap, the mRNA accumulation of GPD and AP17 is higher in the epidermal and subepidermal layers of the mutant embryos and gradually decreases towards the centre (Fig. 4k, o). The expression of CAP is more or less uniform throughout the mutant embryo although parts of the external regions of the scutellum-like structure have a

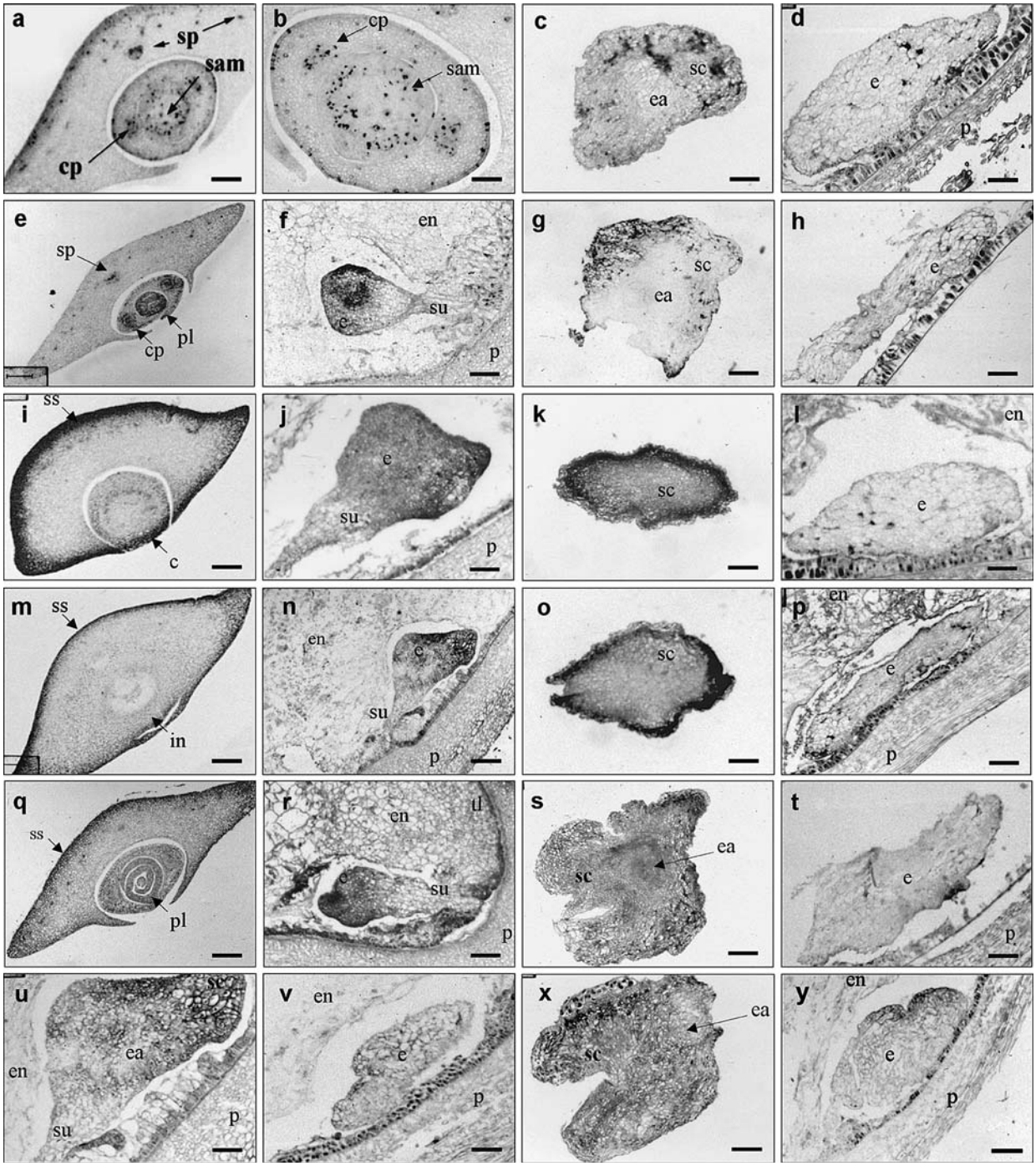

Fig. 4 **a**–**y** Expression of marker genes during embryogenesis in *longcell* mutants. The mRNA accumulation pattern of different genes in sections of immature wild type and *longcell* embryos. **a** Histone 3 gene (*H3*) in transversal section (*TS*) of 20 days after pollination (*dap*) wild type (*WT*) embryo. **b** *H3* in TS of 20 dap WT embryo. **c** *H3* in TS of 20 dap *longcell* (*lc*) embryo. **d** *H3* in longitudinal section (*LS*) of 35 dap *lc* embryo. **e** Elongation factor 1α gene (*EF-1*α) in TS of 20 dap WT embryo. **f** EF-1α in LS of 12 dap *lc* embryo. **g** *EF-1*α in TS of 20 dap *lc* embryo. **h** *EF-1*α in LS of 35 dap *lc* embryo. **i** Glyceraldehyde phosphate dehydrogenase gene (*GPD*) in TS of 20 dap WT embryo. **j** *GPD* in LS of 12 dap *lc* embryo. **k** GPD in TS of 20 dap *lc* embryo. **l** *GPD* in LS of 35 dap *lc* embryo. **m** Acyl carrier protein gene (*AP17*) in TS of 20 dap WT embryo. **n** *AP17* in LS of 12 dap *lc* embryo. **o** *AP17* in TS of 20 dap *lc* embryo. **p** *AP17* in LS of 35 dap *lc* embryo. **q** Clathrin adapter protein gene (*CAP*) in TS of 20 dap WT embryo. **r** *CAP* in LS of 12 dap *lc* embryo. **s** *CAP* in TS of 20 dap *lc* embryo. **t** *CAP* in LS of 35 dap *lc* embryo. **u** *Rab17* in LS of 20 dap *lc* embryo. **v** *Rab17* in LS of 35 dap *lc* embryo. **x** *Rab28* in LS of 20 dap *lc* embryo. **y** *Rab28* in LS of 35 dap *lc* embryo. *c* coleorhyza, *cp* coleoptilar procambium, *ea* embryo axis, *en* endosperm, *in* internode, *p* pericarp, *pl* plumule, *sam* shoot apical meristem, *sc* scutellum, *sp* scutellar procambium, *ss* scutelar subepidermal layer, *e* embryo, *su* suspensor, *tl* endosperm basal transfer layer. *Bars* 50 μm (**f**, **j**, **r**), 100 μm (**b**, **n**), 200 μm (**a**, **e**, **i**, **m**, **q**, **u**), 250 μm (**d**, **h**, **l**, **p**, **t**), 300 μm (**c**, **g**, **k**, **o**, **s**, **v**, **x**, **y**)

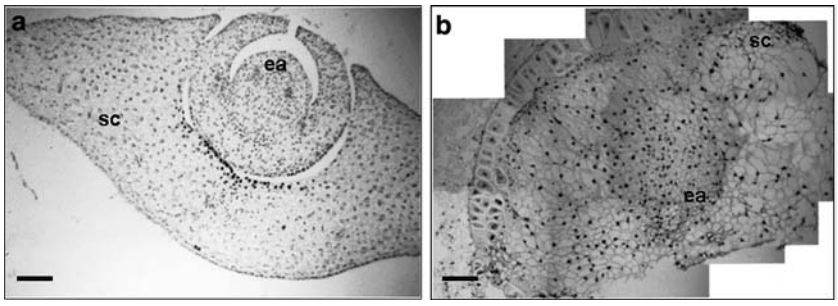

Fig. 5 **a**–**b** Nuclear DNA fragmentation in *longcell* embryos. 34 dap immature embryos were stained using the in situ cell death detection kit (Roche) based on the TUNEL method. **a** Wild type embryo. The *bar* represents 500 μm. **b** *longcell* embryo. The bar represents 200 μm. *sc* scutellum, *ea* embryo axis

higher level of accumulation of mRNA (Fig. 4s). The accumulation of mRNA for all three genes is reduced to a few scattered cells in 35 dap *longcell* embryos (Fig. 4l, p, t).

Finally, we examined the mRNA accumulation of *rab17* and *rab28* genes, which are transcribed in late embryo development and in response to abscisic acid and water stress in embryo and vegetative tissues (Goday et al. 1994; Niogret et al. 1996). As has been described by Goday and col. (1994) initially in the development *rab17* mRNA accumulates in the embryo axis, but as maturation progresses, *rab17* mRNA also accumulates in the scutellum (30 dap). We found that *rab17* mRNA also accumulates in 20 dap *longcell* embryos but, differently to wild type, it is concentrated mainly in the region of the embryo opposite the suspensor (Fig. 4u). On the other hand, as has been described by Niogret et al. (1996), the expression of *rab28* in young wild type embryos is restricted to provascular tissues, and in later stages the most prevalent accumulation occurred in meristem and in the vascular elements of embryo axis and scutellum. The accumulation of *rab28* mRNA is general throughout the *longcell* embryo but it shows some regions of higher intensity in the scutellum-like region (Fig. 4x). The mRNA abundance of both genes is severely reduced in 35 dap *longcell* embryos (Fig. 4v, y).

In situ hybridizations showed little signal in 35 dap embryos for all the genes tested. These results may be because a reduction in the expression of the genes but also because a reduction in the total amount of mRNA in the mutant embryos. RNA extractions on mature *longcell* seeds never succeeded and extractions on 35 and 40 dap seeds always give very few yields comparing with younger mutant seeds. This results suggest a general RNA degradation in *longcell* embryos in the late stages of seed development.

Evidences of cell death in *longcell* seeds

Using agarose gel electrophoresis to examine the integrity of the genomic DNA from mature mutant and wild type embryos extracted from dry seeds, we found that the genomic DNA from *longcell* embryos has a high degree of degradation compared with DNA extracted from wild type embryos (not shown). TUNEL staining has been extensively used for in situ detection of DNA fragmentation sites associated with apoptotic cell death. Nuclei of 34 dap *longcell* embryos had generalized TUNEL staining, compared with wild type embryos of the same age which gave positive TUNEL staining only in the inner layer of the scutellum, next to the coleoptile (Fig. 5a, b).

We examined the expression of genes involved in the execution and regulation of different processes of programmed cell death in plants. The selected genes included different categories:

(a) Nucleases: involved in the degradation of nuclear DNA. We included a gene coding for a nuclease, which we called MEN1, which is homologous to a family of PCD-related S1-type DNAses (Aoyagi et al. 1998).
(b) Proteases: several proteases of different families have been demonstrated as being involved in PCD processes, including aspartic proteases such as phytepsin (Runeberg-Roos and Saarma 1998), serine proteases such as SAS1 (Coffeen and Wolpert 2004) and a group of cysteine-aspartic proteases called metacaspases (McIa, McIb, McIIa, McIIb) (Uren et al. 2000).
(c) Genes involved in the regulation of ROS: ROS (reactive oxygen species) are molecules such as hydroxyl radicals, hydrogen peroxide or superoxide, which have a signalling function in many biological systems, including plant cells. It has been shown that ROS serve as signals to induce changes in gene expression associated with PCD (Apel and Hirt 2004) and the production of ROS may also occur as a consequence of the activation of a pathway leading to cell death. For this reason we also studied the mRNA accumulation of genes associated with antioxidant metabolism, such as a peroxiredoxin (Stacy et al. 1996) and a metallothionein-like coding gene (Ma et al. 1997).

With oligonucleotides specific for each of the genes (Table 1), we examined the mRNA accumulation in wild type and mutant seeds at different stages of development, using RT-PCR assays (Fig. 6). *MEN1* was expressed at higher levels in the *longcell* seeds than in wild type, at the three stages of development tested. Five of the six protease-coding genes also gave higher levels of mRNA in the mutant seeds compared to wild

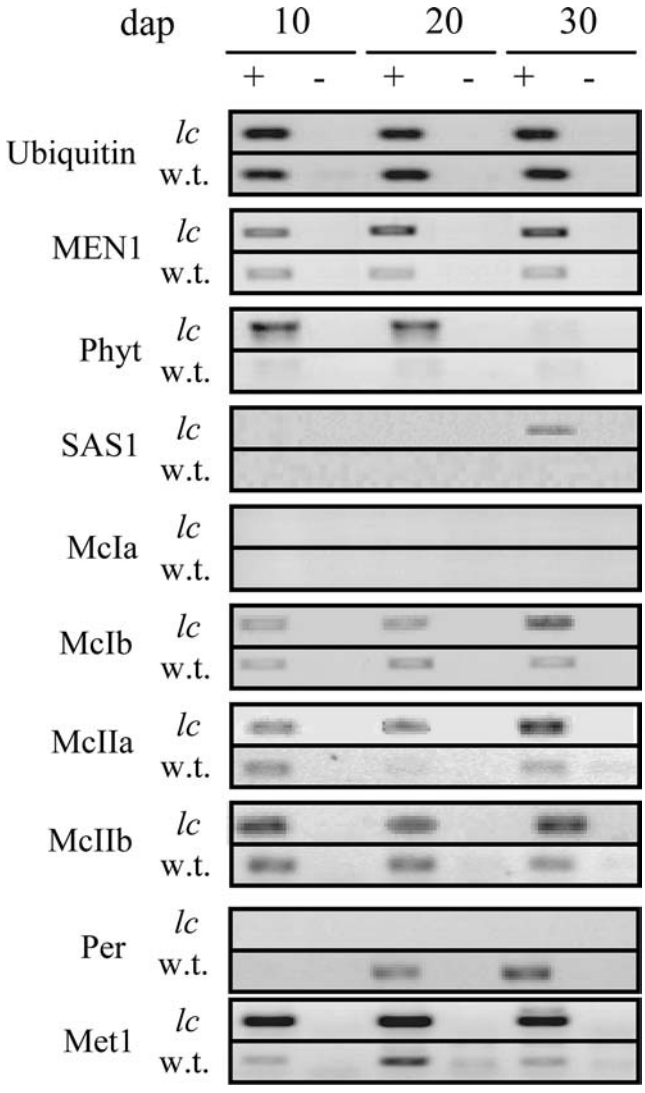

Fig. 6 RT-PCR analysis of the expression profiles of several maize genes putatively involved in PCD processes. Ethidium bromide-stained 1.5% agarose gels showing RT-PCR products. The names of the genes are given in Table 1. *lc* Corresponds to *longcell* kernels and *wt*. to wild type. The numbers on the top correspond to days after pollination. In each case, the size of the bands shown are those expected. The ubiquitin gene was used as control. + corresponds to the RT-PCR assays and – to the negative controls in which the reverse transcriptase was not included in the reaction

type, at different levels and stages of development, and for the only one not differentially expressed, McIa, we were not able to detect mRNA in wild type or in mutant seeds. The expression of hydrolytic genes is typical of PCD processes and is an indication of an active degradation process. Finally, the mRNA accumulation of both genes involved in ROS abundance was altered in *longcell* kernels: the expression of per, a protector against oxidative stress, is reduced in mutant seeds and the mRNA accumulation of *met1*, a gene induced by ROS, was increased at all stages of development studied.

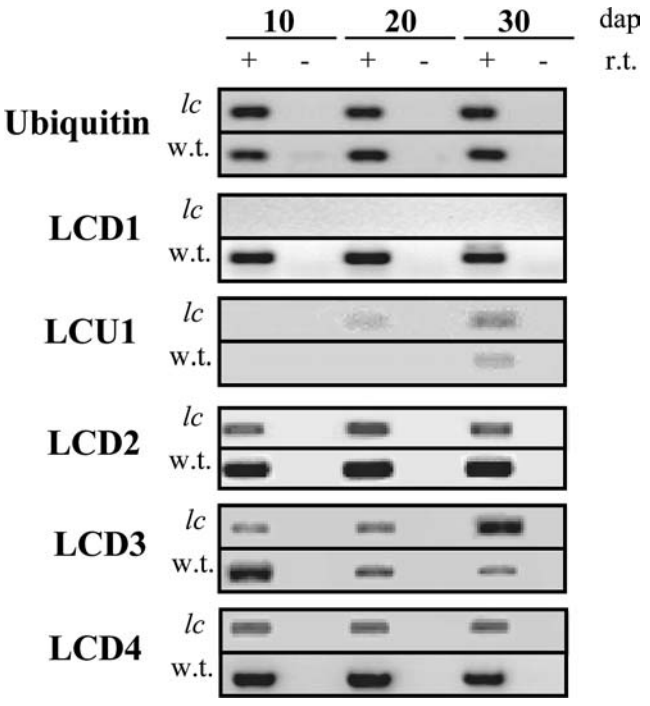

Fig. 7 RT-PCR analysis of the expression profiles of the four maize genes isolated in the DDRT assay. Ethidium bromide-stained 1.5% agarose gels showing RT-PCR products. The names of the genes are given in Table 2. *lc* Corresponds to *longcell* kernels and *wt* to wild type. The numbers on the top correspond to days after pollination. In each case, the size of the bands shown are those expected. The ubiquitin gene was used as control. + corresponds to the RT-PCR assays and – to the negative controls in which the reverse transcriptase was not included in the reaction

Isolation of sequences corresponding to differentially expressed genes in wild type and *longcell* seeds

To identify genes whose expression is altered by *longcell* mutation, we compared the mRNA accumulation profiles of 20 dap maize kernels using mRNA differential display. After the changes in mRNA levels had been confirmed by RT-PCR analysis, the differential display approach resulted in five cDNA clones, varying in length from 411 to 118 bp. The four down-regulated clones were named LCD1, LCD2, LCD3 and LCD4 (for *longcell* down-regulated), and the one up-regulated clone was named LCU1 (for *longcell* up-regulated). An overview of the isolated maize LCD and LCU clones, including GeneBank accession numbers, is given in Table 2. Changes in mRNA levels of the genes corresponding to the LCD and LCU fragments were examined by RT-PCR amplification at three different stages of seed development; 10, 20 and 30 days after pollination (Fig. 7).

LCD1 encodes a myo-inositol 1-phosphate synthase (MIPS), similar to *ZmMIPS1* (Shukla et al. 2004). MIPS protein has been described in many organisms and is the key enzyme in the inositol biosynthetic pathway. In cereal seeds, MIPS is important for the synthesis of phytic acid (myo-inositol-1,2,3,4,5,6-hexa-

kis-phosphate), which is the most important source of phosphorous and other minerals in mature embryos (Raboy et al. 2000). LCD1 was not expressed, or expressed at very low levels, in *longcell* embryos at all stages of development examined (Fig. 7).

LCU1 is 284 nucleotides long and was expressed in *longcell* embryos at 20 and 30 dap, at higher levels than in the wild type. BLAST searches gave high sequence similarity to a rice cytochrome b245 β-chain NADpH oxidase, and an *Arabidopsis* respiratory burst oxidase protein NADpH oxidase (RbohF) (Torres et al. 1998).

LCD2 is 274 bp long. A BLAST nucleotide search gave similarity to a rice pectate lyase-like encoding gene. RT-PCR analysis showed that this gene was down regulated in the mutant seeds relative to the wild type. Pectate lyases (EC: 4.2.2.2) catalyze the eliminative cleavage of de-esterified pectin, a major component in the primary cell walls of many higher plants, and are enzymes involved in the maceration and soft rotting of plant tissues (Turcich et al. 1993).

The LCD3 differentially expressed band encodes a sequence similar to the *Arabidopsis* histone deacetylase 2b (HD2b). These enzymes are involved in the regulation of gene expression via deacetylation of histones, a process that modifies the chromatin from an open gene, active, euchromatin structure to a closed gene, silenced, heterochromatin structure (Struhl 1998). The mRNA accumulation of this gene was lower in the mutant at 10 dap, but higher at 30 dap. In animal systems some histone deacetylases have been implicated in the regulation of apoptosis. Histone deacetylase inhibitors induce apoptosis in a number of malignant cell types (Chobanian et al. 2004) and oxidative stress significantly decreases the activity of a histone deacetylase 2 in cultured cells (Ito et al. 2004).

Finally, LCD4 has sequence similarity to a maize cyclophilin (Cyp) whose expression was lower in the mutant at all three stages of development analyzed. Cyclophilins (EC: 5.2.1.8) are members of a class of proteins with peptidyl-prolyl cis-trans isomerase activity that has been implicated in intracellular protein folding, transport and assembly (Marivet el al. 1995). *Cyp* is expressed in all maize tissues but its mRNA abundance increases during germination, in growing tissues and organs, and in nodes and internodes of adult plants.

Discussion

A large number of maize seed mutants have been isolated (Sheridan and Clark 1993), although only a few have been comprehensively characterized to date. Using a range of microscopy techniques and gene expression assays, we describe here the phenotype of the maize *longcell* mutant. *Longcell* is a lethal and recessive defective-kernel mutant that has a distorted embryo and a reduced endosperm (Graziano et al. 2003).

Expression of germination-specific genes during embryogenesis

One altered aspect of the *longcell* mutant is the induction during embryogenesis of genes which, under normal conditions, are only expressed after germination. For convenience, embryogenesis has been divided into modules separated in time, but, in fact, embryogenesis and germination are parts of a continuous developmental process, only temporally interrupted by quiescence (Kaplan and Cooke 1997). The transition from embryogenesis to germination is regulated by many transcription factors. Genetic alterations in these factors produce mutants in which the pathway of embryogenesis and germination is affected, as occurs in *leafy cotyledon*1, and *fusca3* in *Arabidopsis* and *abscisic acid-insensitive* mutants in maize and Arabidopsis (Brocard-Gifford et al. 2003). For example, an increase in α-amylase activity was observed in *viviparous1* seeds (Young and Gallie 2000). Alterations in the embryogenesis program in *longcell* could easily affect this complex regulation and induce precocious expression of genes from the post-germination programme

Cell death in *longcell* embryos is genetically regulated

Cell death is often linked to embryo mutants (Clark and Sheridan 1986) and is induced in *longcell* embryos. Cell death may be through necrosis or PCD. Necrosis is a non-physiological, non-regulated process, whereas PCD is a genetically regulated process and requires the activation or inactivation of several genes and proteins (Pennell and Lamb 1997). Cell death in embryo defective mutants has usually been considered necrotic (Clark and Sheridan 1986). In the case of the *longcell* mutant, death of the embryo involves a genetic regulation because it is accompanied by the induction of expression of genes coding for hydrolytic enzymes, including, at least, different classes of proteases and a nuclease. Moreover, we also detected nuclear TUNEL staining in dying embryos, which is an indication that death proceeds in a regulated manner. There were also changes in the expression of oxidation-related genes, and reactive oxygen species (ROS) are often involved in the regulation of PCD processes (Apel and Hirt 2004). All these data indicate that the death of *longcell* embryos is not necrotic.

In animals, some data demonstrate the linked regulation between cell death and cell division (Burgering and Kops 2002). In plants, this relationship is not so well studied but, for example, elicitor induction of cell death during the HR response in tobacco BY-2 cells depends on the cell cycle (Kadota et al. 2004). The abnormal development in *longcell* embryos could alter the normal induction of PCD, leading to generalized cell death. The opposite phenomenon, the inhibition of cell death, also produces abnormal phenotypes, as has been suggested by Consonni et al. (2003) for certain maize mutants.

Cell elongation and body pattern formation in *longcell* mutants

Maybe the most striking characteristics of the *longcell* mutant is the apparent disruption of the balance between elongation and division that produces enlarged, tubular cells in the scutellum-like structure. The production of enlarged, tubular cells could be due to an increase in the cell expansion rate, but depression or absence of cytokinesis could produce a similar result. The abnormal cells in *longcell* embryos elongate, suggesting that they are not impaired in the synthesis and transport of new cell wall components. The expression of the clathrin adapter protein involved in vesicle transport from Golgi apparatus, and of the acyl carrier protein involved in lipid biosynthesis is not disabled in the mutant, at least in early and mid-embryogenesis. On the other hand, the elongated cells are tubular in shape and not spherical, indicating that some of the cortical microtubule arrays are present and constrain the direction of cell growth (Whittington et al. 2001) which leads to one possible hypothesis, that *longcell* embryos could be defective in cytokinesis.

Arabidopsis mutants affected in cytokinesis have enlarged, tubular cells (Mayer and Jürgens 2004). These mutants also have rough surfaces and alterations in cellular differentiation, but the general body plan is usually preserved (Söllner et al. 2002). In some cases, although cell division is blocked, embryos remain alive for a long time. For example, the *Arabidopsis pilz* cytokinesis-defective mutant is blocked in cell division at a very early stage but the cells stay alive, express cell-cycle regulators and maintain their apical-basal cell fates (Mayer et al. 1999). The stage of development and the organs in which cytokinesis is blocked are variable, and consequently the phenotypes produced may range from embryo lethality to effects in only some specific organs. For example, in the *Arabidopsis pilz* mutant, cytokinesis is blocked at very early stages of embryo development (Mayer et al. 1999), but in the pea *cyd* mutant, cytokinesis defects are predominant in the developing cotyledons (Liu et al. 1995). Another characteristic of many cytokinesis-defective mutants is the variability of phenotypes produced by the same mutation. For example, disruption of an *Arabidopsis prolifera* gene leads to a cytokinesis defect that produces embryo lethality, but the arrest in embryo development is at a variety of stages (Holding and Springer 2002). Söllner et al. (2002) found similar variability in the *Arabidopsis club* mutant and suggested that the first appearance of cytokinesis defects during development may be stochastically.

Some maize cytokinesis-defective mutants have been described. For example, *tangled1* and *warty1* mutants are affected in the cytokinesis in leaves (Smith et al. 2001) and, although the genes producing the mutations are not known, it has been suggested that some maize *dek* and *emb* mutants are also affected in cytokinesis (Consonni et al. 2003). As well as the presence of enlarged tubular cells, several features of *longcell* are similar to those observed in cytokinesis-defective mutants. For example, *longcell* embryos have rough surfaces, abnormalities in cell differentiation, preservation of the general body pattern, expression of genes involved in basic metabolism and phenotype variability. They are affected only, or mainly, in certain organs and they are apparently able to develop normally up to a certain developmental stage. In view of this, we postulate that cytokinesis is impaired or reduced in *longcell* embryos. The changes in the accumulation of storage molecules, the activation of the expression of genes that in normal conditions are only expressed after germination, and the induction of cell death in the embryo are probably secondary effects of the cytokinesis alterations.

Acknowledgments In Memoriam: Dr Virginia Stiefel. This work was carried out thanks to grants BIO2001-1721 and BIO2004-01577 from Plan Nacional de Investigación Científica y Técnica and a grant from the program MAZE, European Union, and within the framework of Centre de Referència de Biotecnologia de la Generalitat de Catalunya. M.B. was the recipient of a fellowship of the CIRIT (Generalitat de Catalunya). C.M.V. is the recipient of a "Ramon y Cajal" contract from the Spanish Ministry of Science. We thank Pilar Fontanet for technical support.

References

Aoyagi S, Sugiyama M, Fukuda H (1998) BEN1 and ZEN1 cDNAs encoding S1-type DNases that are associated with programmed cell death in plants. FEBS Lett 429:134–138

Apel K, Hirt H (2004) Reactive oxygen species: metabolism, oxidative stress, and signal transduction. Annu Rev Plant Biol 55:373–399

Bastida M, Puigdomenech P (2002) Specific expression of ZmPRL, the maize homologue of MCM7, during early embryogenesis. Plant Sci 162:97–106

Bradford MM (1976) A rapid and sensitive for the quantitation of microgram quantitites of protein utilizing the principle of protein-dye binding. Anal Bioch 72:248–254

Brocard-Gifford IM, Lynch TJ, Finkelstein RR (2003) Regulatory networks in seeds integrating developmental, abscisic acid, sugar, and light signaling. Plant Physiol 131:78–92

Brzobohaty B, Moore I, Kristoffersen P, Bako L, Campos N, Schell J, Palme K (1993) Release of active cytokinin by a beta-glucosidase localized to the maize root meristem. Science 262:1051–1054

Burgering BMT, Kops GJPL (2002) Cell cycle and death control: long live forkheads. Trends Bioch Sci 27:352–360

Chandler PM, Zwar JA, Jacobsen JV, Higgins TJV, Inglis AS (1984) The effects of gibberellic acid and abscisic acid on α-amylase mRNA levels in barley aleurone layers studies using an α-amylase cDNA clone. Plant Mol Biol 3:407–418

Chobanian NH, Greenberg VL, Gass JM, Desimone CP, Van Nagell JR, Zimmer SG (2004) Histone deacetylase inhibitors enhance paclitaxel-induced cell death in ovarian cancer cell lines independent of p53 status. Anticancer Res 24:539–545

Clark JK, Sheridan WF (1986) Developmental profiles of the maize embryo-lethal mutants dek22 and dek23. J Hered 77:83–92

Coffeen WC, Wolpert TJ (2004) Purification and characterization of serine proteases that exhibit caspase-like activity and are associated with programmed cell death in *Avena sativa*. Plant Cell 16:857–873

Consonni G, Aspesi C, Barbante A, Dolfini S, Giuliani C, Giulini A, Hansen S, Brettschneider R, Pilu R, Gavazzi G (2003) Analysis of four maize mutants arrested in early embryogenesis reveals an irregular pattern of cell division. Sex Plant Reprod 15:281–290

de Framond AJ (1991) A metallothionein-like gene from maize (*Zea mays* L). Cloning and characterization. FEBS Lett 290:103–106

Dellaporta SL, Moreno SA (1994) Gene tagging with Ac/Ds elements in maize. In: Freeling M, Walbot V (eds) The maize handbook. Springer, Berlin Heidelberg New York, pp 219–234

Fu S, Meeley R, Scanlon J (2002) *Empty pericarp2* encodes a negative regulator of the heat shock response and is required for maize embryogenesis. Plant Cell 14:3119–3132

Gallie DR (2004) Programmed cell death during seed development and germination. In: Gray J (ed) Programmed cell death in plants. Blackwell, Amsterdam pp 44–70

Geetha KB, Lending CR, Lopes MA, Wallace JC, Larkins BA (1991) Opaque-2 modifiers increase gamma-zein synthesis and alter its spatial distribution in maize endosperm. Plant Cell 3:1207–1219

Goday A, Jensen AB, Culiañez-Maciá FA, Alba MM, Figueras M, Serratosa J, Torrent M, Pagès M. (1994) The maize abscisic acid-responsive protein Rab17 is located in the nucleus and interacts with nuclear localization signals. Plant Cell 6:351–360

Graziano E, Bastida M, Stiefel V, Puigdomenech P (2003) *Longcell*, a mutant from maize producing a distorted embryo and generalized cell death. In: Nicolas G, Bradford KJ, Côme D, Pritchard HW (eds) The biology of seeds, recent research advances. CABI Publishing. Oxon, pp 25–32

Halick JV, Keneaster KK (1956) The use of a starch-iodine-blue test as a quality indicator of white milled rice. Cereal Chem 33:315–319

Holding DR, Springer PS (2002) The *Arabidopsis* gene PROLIFERA is required for proper cytokinesis during seed development. Planta 214:373–382

Ingram GC, Boisnard-Lorig C, Dumas C, Rogowsky PM (2000) Expression patterns of genes encoding HD-ZipIV homeo domain proteins define specific domains in maize embryos and meristems. Plant J 22:401–414

Ito K, Hanazawa T, Tomita K, Barnes PJ, Adcock IM (2004) Oxidative stress reduces histone deacetylase 2 activity and enhances IL-8 gene expression: role of tyrosine nitration. Biochem Biophys Res Commun 315:240–245

Jürgens G (2001) Apical-basal pattern formation in *Arabidopsis* embryogenesis. EMBO J 20:3609–3616

Kadota Y, Watanabe T, Fujii S, Higashi K, Sano T, Nagata T, Hasezawa S, Kuchitsu K (2004) Crosstalk between elicitor-induced cell death and cell cycle regulation in tobacco BY-2 cells. Plant J 40:131–142

Kaplan DR, Cooke TJ (1997) Fundamental concepts in the embryogenesis of dicotyledons: a morphological interpretation of embryo mutants. Plant Cell 9:1903–1919

Keller T, Damude HG, Werner D, Doerner P, Dixon RA, Lamb C (1998) A plant homolog of the neutrophil NADPH oxidase gp91phox subunit gene encodes a plasma membrane protein with Ca2+ binding motifs. Plant Cell 10:255–266

Lam E, Greenberg J (2000) Cell death: the 'Yin' path in the balancing act of the life cycle. Plant Mol Biol 44:vii–viii

Langdale JA (1994) In situ hybridization. In: Freeling M, Walbot V (eds) The maize handbook. Springer, Berlin Heidelberg New York, pp 165–180

Lid SE, Gruis D, Jung R, Lorentzen JA, Ananiev E, Chmberlein M, Niu X, Meeley R, Nichols S, Olsen OA (2002) The *defective kernel 1* (*dek1*) gene required for aleurone cell development in the endosperm of maize grains encodes a membrane protein of the calpain gene superfamily. Proc Natl Acad Sci USA 99:5460–5465

Liu CM, Johnson S, Wang TL (1995) cyd, a mutant of pea that alters embryo morphology is defective in cytokinesis. Dev Genet 16:312–331

Lopez-Becerra E, Puigdomenech P, Stiefel V (1998) A gene coding for a malic enzyme expressed in the embryo root epidermis from *Zea mays* L (Accession No. AJ224847). Plant Physiol 127:331–334

Ma M, Tsang WK, Lau PS, Wong YS (1997) Cloning and sequencing of the metallothionein-like cDNA from *Festuca rubra* cv Merlin. Plant Physiol 114:1136

Ma Z, Dooner HK (2004) A mutation in the nuclear-encoded plastid ribosomal protein S9 leads to early embryo lethality in maize. Plant J 37:92–103

Magnard JL, Heckel T, Massonneau A, Wisniewski JP, Cordelier S, Lassagne H, Perez P, Dumas C, Rogowsky PM (2004) Morphogenesis of maize embryos requires ZmPRPL35-1 encoding a plastid ribosomal protein. Plant Physiol 134:649–663

Marivet J, Frendo P, Burkard G (1995) DNA sequence analysis of a cyclophilin gene from maize: developmental expression and regulation by salicylic acid. Mol Gen Genet 247:222–228

Mayer U, Jürgens G (2004) Cytokinesis: lines of division taking shape. Curr Opin Plant Biol 7:599–604

Mayer U, Herzog U, Berger F, Inze D, Jurgens G (1999) Mutations in the pilz group genes disrupt the microtubule cytoskeleton and uncouple cell cycle progression from cell division in *Arabidopsis* embryo and endosperm. Eur J Cell Biol 78:100–108

Meinke DW, Meinke LK, Showalter TC, Schissel AM, Mueller LA, Tzafrir I (2003) A sequence-based map of *Arabidopsis* genes with mutant phenotypes. Plant Physiol 131:409–418

Niogret MF, Culiañez-Maciá FA, Goday A, Pagès M (1996) Expression and cellular localization of *rab28* mRNA and Rab28 protein during maize embryogenesis. Plant J 9:549–557

Pennell RI, Lamb C (1997) Programmed cell death in plants. Plant Cell 9:1157–1168

Raboy V, Gerbasi PF, Young KA, Stoneberg SD, Pickett SG, Bauman AT, Murthy PP, Sheridan WF, Ertl DS (2000) Origin and seed phenotype of maize low phytic acid 1-1 and low phytic acid 2-1. Plant Physiol 124:355–368

Roca R, Stiefel V, Puigdomenech P (1998) Characterization of the sequence coding for the clathrin coat assembly protein AP17 (2) associated with the plasma membrane from *Zea mays* L and constitutive expression of its gene. Gene 208:67–72

Runeberg-Roos P, Saarma M (1998) Phytepsin, a barley vacuolar aspartic proteinase, is highly expressed during autolysis of developing tracheary elements and sieve cells. Plant J 15:139–145

Sheridan WF, Clark JK (1993) Mutational analysis of morphogenesis of the maize embryo. Plant J 3:347–358

Shukla S, VanToai TT, Pratt RC (2004) Expression and nucleotide sequence of an INS (3) P1 synthase gene associated with low-phytate kernels in maize (*Zea mays* L.). J Agric Food Chem 52:4565–4570

Söllner R, Glasser G, Wanner G, Somerville CR, Jurgens G, Assaad FF (2002) Cytokinesis-defective mutants of *Arabidopsis*. Plant Physiol 129:678–690

Smith LG, Gerttula SM, Han S, Levy J (2001) Tangled1: a microtubule binding protein required for the spatial control of cytokinesis in maize. J Cell Biol 152:231–236

Stacy RA, Munthe E, Steinum T, Sharma B, Aalen RB (1996) A peroxiredoxin antioxidant is encoded by a dormancy-related gene, Per1, expressed during late development in the aleurone and embryo of barley grains. Plant Mol Biol 31:1205–1216

Struhl K (1998) Histone acetylation and transcriptional regulatory mechanisms. Genes Dev 12:599–606

Torres MA, Onouchi H, Hamada S, Machida C, Hammond-Kosack KE, Jones JD (1998) Six *Arabidopsis thaliana* homologues of the human respiratory burst oxidase (gp91phox). Plant J 14:365–370

Turcich MP, Hamilton DA, Mascarenhas JP (1993) Isolation and characterization of pollen-specific maize genes with sequence homology to ragweed allergens and pectate lyases. Plant Mol Biol 23:1061–1065

Uren AG, O'Rourke K, Aravind LA, Pisabarro MT, Seshagiri S, Koonin EV, Dixit VM (2000) Identification of paracaspases and metacaspases: two ancient families of caspase-like proteins, one of which plays a key role in MALT lymphoma. Mol Cell 6:961–967

Whittington AT, Vugrek O, Wei KJ, Hasenbein NG, Sugimoto K, Rashbrooke MC, Wasteneys GO (2001) MOR1 is essential for organizing cortical microtubules in plants. Nature 411:610–613

Young TE, Gallie DR (2000) Programmed cell death during endosperm development. Plant Mol Biol 44:283–301

Young TE, DeMason DA, Close TJ (1994) Cloning of an alpha-amylase cDNA from aleurone tissue of germinating maize seed. Plant Physiol 105:759–760

Zhou C, Labbe H, Sridha S, Wang L, Tian L, Latoszek-Green M, Yang Z, Brown D, Miki B, Wu K (2004) Expression and function of HD2-type histone deacetylases in *Arabidopsis* development. Plant J 38:715–724